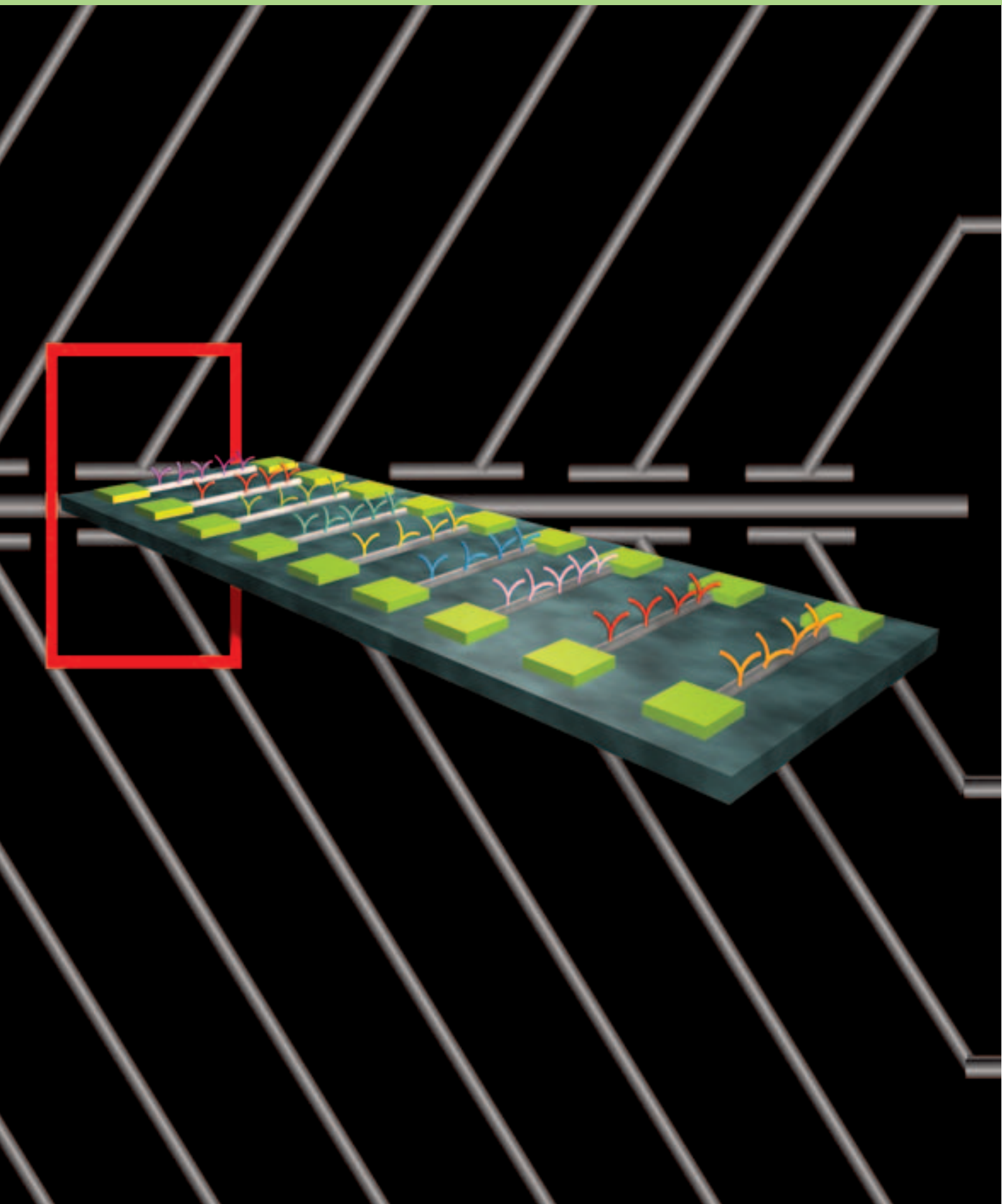

NANOWIRE-BASED BIOSENSORS

Fernando Patolsky

Gengfeng Zheng

Charles M. Lieber

HARVARD UNIVERSITY

Devices based on nanowires are emerging as a powerful platform for the direct detection of biological and chemical species, including low concentrations of proteins and viruses.

Detection and quantification of biological and chemical species are critical to many areas of health care and the life sciences, from diagnosing disease to the discovery and screening of new drug molecules. Central to detection is the transduction of a signal associated with the selective recognition of a species of interest. Several approaches have been reported for the detection of biological molecules, including ELISAs (*1*), surface plasmon resonance (SPR; *2*), nanoparticles (*3*), chemically sensitive field-effect transistors (CHEMFETs; *4*, *5*), microcantilevers (*6*), and carbon nanotubes (*7*, *8*). Although advances have been made with each of these methods, none has yet demonstrated the combination of features required for rapid, highly sensitive multiplexed detection of biomolecules.

Nanostructures, such as nanowires (NWs) (*9*–*12*) and nanocrystals (*13*, *14*), offer new and sometimes unique opportunities to develop novel sensors. The diameters of these nanostructures are comparable to those of the biological and chemical species being sensed. Therefore, they represent excellent primary transducers for producing signals that ultimately interface to macroscopic instruments. In particular, inorganic NWs and nanocrystals exhibit highly reproducible electrical (*11*, *15*–*22*) and optical (*13*, *14*) properties.

The size-tunable colors of semiconductor nanocrystals together with their highly robust emission properties offer advantages over conventional organic molecular dyes for labeling and optical-based detection of biological species (*13*, *14*). The combination of tunable conducting properties of semiconducting NWs (*16*–*20*) and the ability to bind analytes on their surface yields direct, label-free electrical readout, which is exceptionally attractive for many applications (*23*–*31*). We discuss representative examples in which these new sensors have been used for detecting a wide range of biological and chemical species. Moreover, we show how advances in the integration of nanoelectronic devices enable multiplexed detection and thereby provide a clear pathway for diverse and exciting applications.

NW field-effect sensors

Detectors based on semiconductor NWs are configured as field-effect transistors (FETs), which exhibit a conductivity change in response to variations in the electric field or potential at the surface (*11*, *23*, *25*). In a standard FET, a semiconductor, such as p-type silicon (p-Si), is connected to metal source and drain electrodes through which a current is injected and collected, respec-

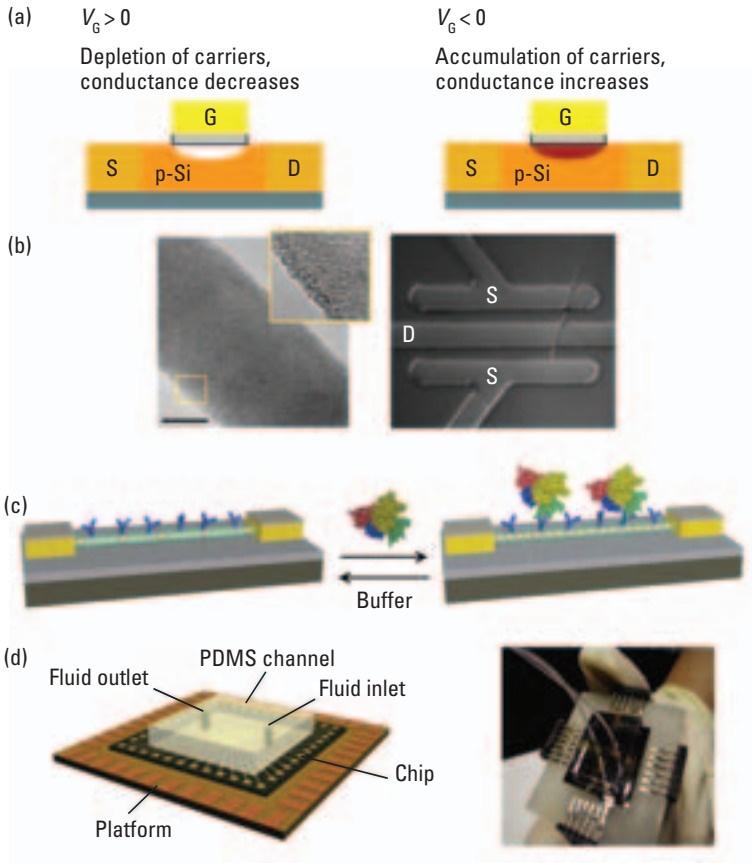

FIGURE 1. NW FET sensors.

(a) Schematic of a p-type FET device. S, source; D, drain; and G, gate electrodes; V_G, gate voltage. (b) (left) Transmission electron microscope images of a 20-nm-diam single-crystal SiNW and (right) an optical image of a SiNW device. (c) Schematic of a NW device configured as a sensor with antibody receptors (blue); binding of a protein with a net negative charge results in an increase in the conductance. (d) Prototype NW sensor biochip with integrated microfluidic sample delivery.

tively (Figure 1a). The conductance of the semiconductor between the source and the drain is switched on and off by a third, gate electrode that is capacitively coupled through a thin dielectric layer (*32*). In the case of a p-Si or other p-type semiconductor, applying a positive gate voltage depletes carriers and reduces the conductance, whereas applying a negative gate voltage leads to an accumulation of carriers and increases the conductance. The dependence of the conductance on gate voltage makes FETs natural candidates for electrically based sensing, because the electric field resulting from the binding of a charged species to the gate dielectric is analogous to the effect of applying a voltage with a gate electrode. This idea for sensing with FETs was introduced several decades ago for CHEMFETs (*4*, *5*, *33*, *34*), although the limited sensitivity of previous planar devices has precluded them from having a large impact as chemical or biological sensors.

Semiconductor NWs composed of silicon or other materials also can function as FET devices (*11*, *16*, *18*–*22*). Silicon NWs (SiNWs), one of the best-characterized examples of semiconducting NWs, can be prepared as single-crystal structures with diameters as small as 2–3 nm (*9*–*11*, *35*). They can be prepared as p- or n-type materials and configured as FETs (Figure 1b) that exhibit electrical performance characteristics comparable to or better than those achieved in the microelectronics industry for planar silicon devices (*18*, *20*, *21*). These characteristics are also highly reproducible because they can be well controlled during growth, in contrast to the properties of carbon nanotubes (*20*).

The high-performance switching characteristics of SiNWs are among the most important factors that affect sensitivity. The 1D morphology of these nanoscale structures overcomes the sensitivity limitations of earlier planar FET sensors. The binding of biomolecules to the surface of the NW leads to depletion or accumulation of carriers in the bulk of the nanometer-diameter structure, versus only the surface region of a planar device (*23*). This unique feature of semiconductor NWs provides sufficient sensitivity to enable the detection of single viruses (*28*) and of single molecules in solution. However, because these are field-effect devices, detection sensitivity depends on the ionic strength of the solution.

A general sensing device can be configured from high-performance NW FETs by linking NW receptor groups that recognize specific molecules to the surface of the NW (Figure 1c). Because SiNWs have native oxide coatings, this receptor linkage is straightforward; extensive data exist for the chemical modification of silicon oxide or glass surfaces from planar chemical and biological sensors (*36*). When the sensor device with surface receptors is exposed to a solution containing a macromolecule, like a protein, that has a net negative (or positive) charge in aqueous solution, specific binding will lead to an increase (or decrease) in the surface negative charge and an increase (or decrease) in conductance for a p-type NW device. As a proof of concept, we have developed a flexible integrated NW sensor platform that incorporates SiNWs with well-defined p- or n-type doping; source and drain electrodes that are insulated from the aqueous environment, so that only processes occurring at the SiNW surface contribute to electrical signals; and a mated microfluidic channel for delivery of solutions (*28*, *29*; Figure 1d).

The prototypical case of pH

The first demonstration of the use of NW field-effect devices to detect analytes in solution occurred in 2001 with the sensing of hydrogen-ion concentration or pH (*23*). Figure 2a illustrates a p-SiNW device that was transformed into a pH sensor by modifying the silicon oxide surface with 3-aminopropyltriethoxysilane; this yielded amino groups at the NW surface along with the naturally occuring silanol groups of the oxide on the NW surface. The amino and silanol moieties functioned as receptors for hydrogen ions by undergoing protonation and deprotonation reactions that changed the charge density on the surface of the NW. Significantly, p-SiNW devices modified in this way (Figure

2b) exhibited stepwise increases in conductance as the solution pH was increased stepwise from 2 to 9. (The solution was delivered through a microfluidic device.) The nearly linear increase in conductance as pH increased is desirable in a sensor, and it resulted from the presence of two distinct receptor groups that underwent protonation and deprotonation reactions over different pH ranges. From a mechanistic standpoint, the increase in conductance with rising pH was consistent with a decrease of the surface positive charge (increase of the negative charge), which "turned on" the p-type FET via the accumulation of carriers.

The key role that the surface receptor played in defining the hydrogen-ion response was further tested by recording NW conductance versus pH for devices in which the silicon oxide surface layer was not modified with 3-aminopropyltriethoxysilane (Figure 2c). In this case, only the silanol group can function as a receptor for hydrogen ions. Measurements of the conductance as a function of pH showed two different response regimes (Figure 2d). This was not the case with NW surfaces that contained both amino and silanol receptors; then, the conductance change was small at low pH (2–6) but larger and comparable to Figure 2b for high pH (6–9). Moreover, the pH-dependent changes in conductance were in excellent agreement with previous measurements of the pH-dependent surface charge density derived from silica (*37*). This comparison clearly demonstrated that the sensing mechanism was indeed due to a field effect.

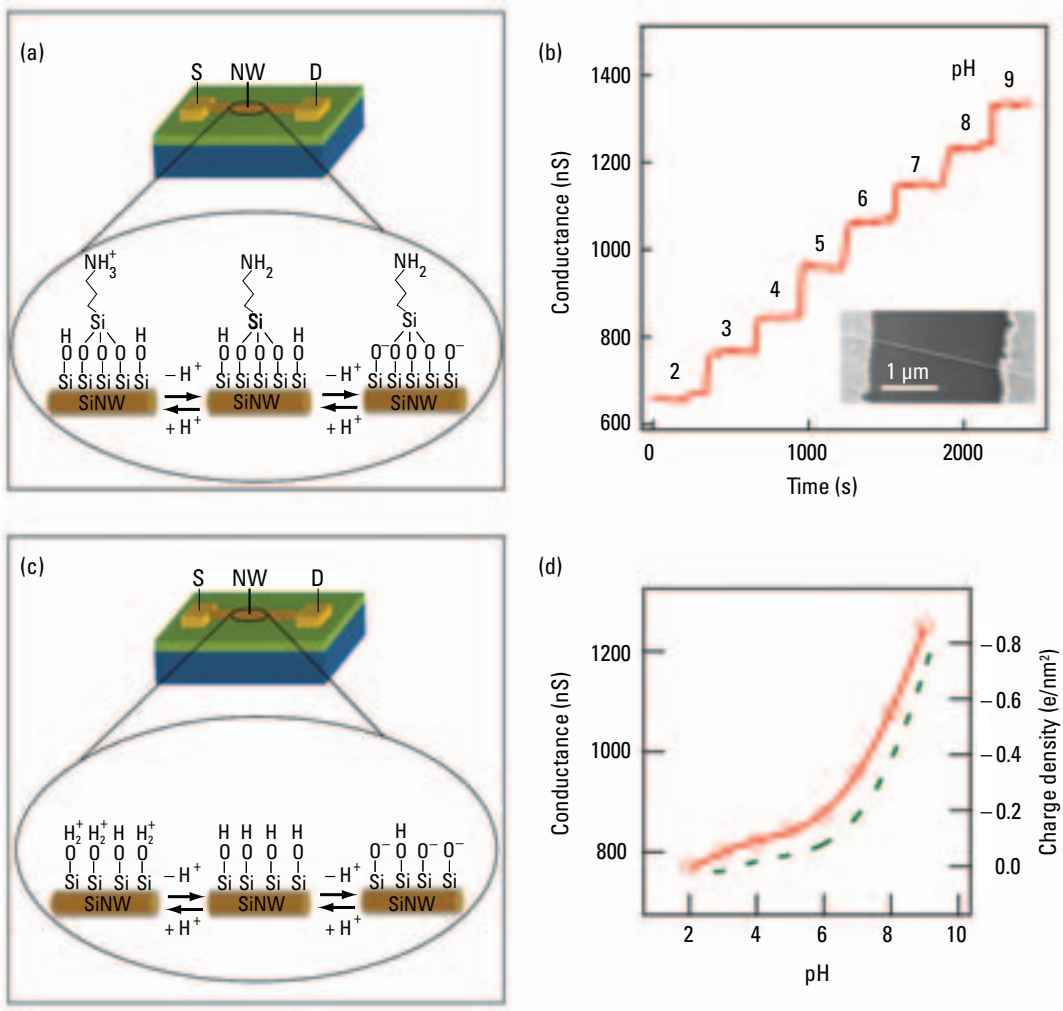

FIGURE 2. NW pH sensors.

(a) Schematic of an amino-functionalized NW device and the protonation and deprotonation equilibria that change the surface charge state. (b) Changes in NW conductance as the pH of the solutions delivered to the sensor varies from 2 to 9. (c) Schematic of an unmodified NW sensor containing silanol groups and the protonation and deprotonation equilibria. (d) Conductance of an unmodified SiNW device (red) vs pH. The dashed green curve is a plot of the surface charge density for silanol groups on silica.

A tool for drug discovery

Identification of organic molecules that bind specifically to proteins is central to the discovery and development of new pharmaceuticals and to chemical genetic approaches for elucidating complex pathways in biological systems (*38*). An example is the identification of molecular inhibitors of tyrosine kinases, which are proteins that mediate signal transduction in mammalian cells through the phosphorylation of a tyrosine residue of a substrate protein via adenosine triphosphate (ATP; *39*). Deregulation of the phosphorylation process has been linked to several diseases, including cancer (*39*). To configure NW sensor devices to screen inhibitors, we linked the Ab1 tyrosine kinase to the surface of SiNW FETs and investigated the binding of ATP and the competitive inhibition of ATP binding with organic molecules, such as the drug Gleevec (*27*). In this configuration, binding (or inhibition of binding) of the negatively charged ATP to Ab1 linked at the SiNW surface was detected simply as an increase (or decrease) in the conductance of the p-type NW device; this is analogous to the pH studies discussed earlier.

Data recorded from Ab1-modified p-SiNW devices showed reversible, concentration-dependent increases in conductance upon introduction of ATP solutions (Figures 3a and 3b). The increases in conductance were consistent with the binding of negatively charged ATP to Ab1 (*27*). Of perhaps greater importance

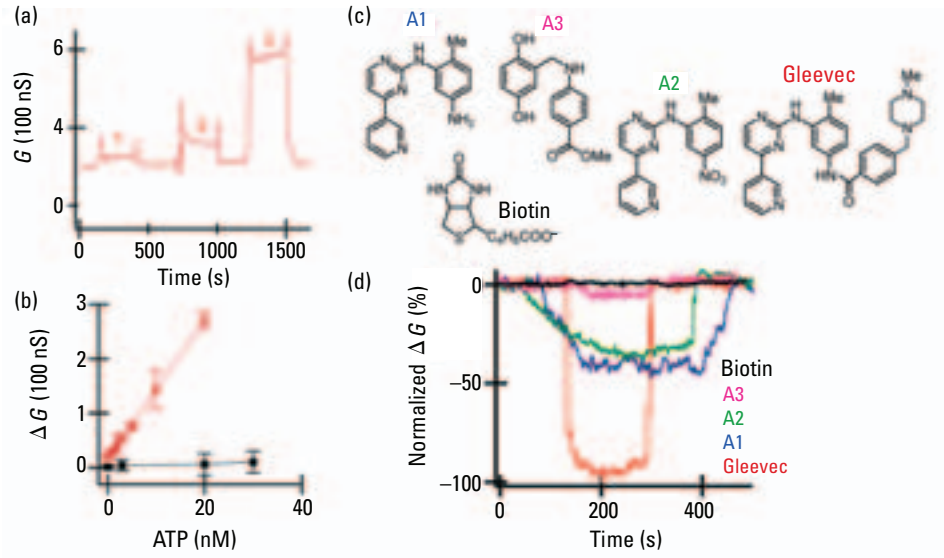

FIGURE 3. NW sensors for drug discovery.

(a) Time-dependent conductance *G* curve at different ATP concentrations for a NW modified with the kinase Ab1. Regions 1, 2, and 3 correspond to 0.1, 3, and 20 nM ATP, respectively. Arrows indicate the points where the solution was changed. (b) Δ*G* vs ATP concentration for an Ab1-modified SiNW (red) and a SiNW without Ab1 (black). (c) Structures of four small molecules that competitively inhibit the binding of ATP to Ab1 and the control molecule biotin. (d) Normalized conductance data showing the relative inhibition of ATP binding.

has been the ability to quantify inhibition of ATP binding by Gleevec and other small molecules (Figure 3c). Plots of the normalized conductance recorded from Ab1-modified p-SiNW devices showed reversible decreases in conductance due to competitive inhibition of ATP binding by the different small molecules (Figure 3d). Notably, the conductance decreases at constant small-molecule concentrations depend strongly on the molecular structures, with Gleevec > A1 > A2 > A3; the control molecule, biotin, shows essentially no change above background, as expected (*27*). These studies demonstrate the substantial advantages of NW detectors over existing methods for rapid, direct, and high-sensitivity analysis of binding and inhibition with a minimal amount of protein receptor.

Detection of DNA and DNA enzymatic processes

Biological macromolecules, such as nucleic acids and proteins, are generally charged in aqueous solution and can be readily and selectively detected when appropriate receptors are linked to the NW's active surface. SiNW field-effect devices have been used to detect single-stranded DNA: The binding of this negatively charged polyanionic macromolecule to p-type NW surfaces leads to an increase in conductance (*26*). Recognition of the DNA target molecule was carried out with complementary single-stranded sequences of peptide nucleic acids (PNAs; *40*). PNA was used as the receptor because the uncharged PNA molecule has a greater affinity and stability than corresponding DNA recognition sequences at low ionic strength (where NW sensitivity is greater).

Studies of p-SiNW devices modified with a PNA receptor designed to recognize the wild-type sequence versus the ΔF508 mutation site in the cystic fibrosis transmembrane receptor gene showed that the conductance increased after addition of a 60-fM wild-type DNA sample solution. The rise in conductance for the p-SiNW device was consistent with an increase in negative surface charge density associated with binding of negatively charged DNA at the surface. Moreover, careful control experiments showed that the binding response was specific to the wild-type sequence and that a sample sequence bearing the ΔF508 mutation did not show this stable change in conductance (*26*). Although this mutation is just one of many that lead to cystic fibrosis, the type of sequence specificity demonstrated in this experiment is critical for the development of the NW devices that can detect genetic modifications associated with disease.

Several other features of NW-based DNA sensors deserve mention. First, the studies of the conductance change versus the concentration of the target sequence demonstrated that direct electrical detection was possible down to at least the 10-fM level. This detection limit is 2–5 orders of magnitude better than that demonstrated by existing real-time measurements, including SPR (*40*), nanoparticle-enhanced SPR (*41*), and the quartz-crystal microbalance (*42*), for DNA detection. The high sensitivity of NW sensors is expected because the diameters of these sensors are comparable to the size of the DNA molecules being sensed and because significant signal changes will be induced by the binding of a small number of DNA molecules on the surface of a single NW. Second, independent SiNW devices exhibit very similar changes in conductance with increasing DNA concentration. Device-to-device reproducibility is an important validation of the potential of SiNWs for development as integrated sensors.

The potential of NW arrays as activity-based diagnostic tools is illustrated in an orthogonal nucleic-acid-based marker assay involving the detection of the activity and inhibition of telomerase, a eukaryotic ribonucleoprotein complex that catalyzes the addition of the telomeric repeat sequence TTAGGG to the ends of chromosomes (*29*, *43*, *44*). Telomerase is inactive in most normal somatic cells but active in ≥80% of known human cancers (*45*); thus, it is a potential marker and therapeutic target for cancer detection and treatment. The NW telomerase assay (Figure 4a) is remarkably simple and detects the presence or absence of telomerase simply by monitoring the NW conductance after delivery of a sample cell extract to the device array (*29*). Addition of deoxynucleotide triphosphates (dNTPs) further allows for monitoring of activity through an increase in conductance due to the incorporation of negatively charged nucleotides near the NW surface.

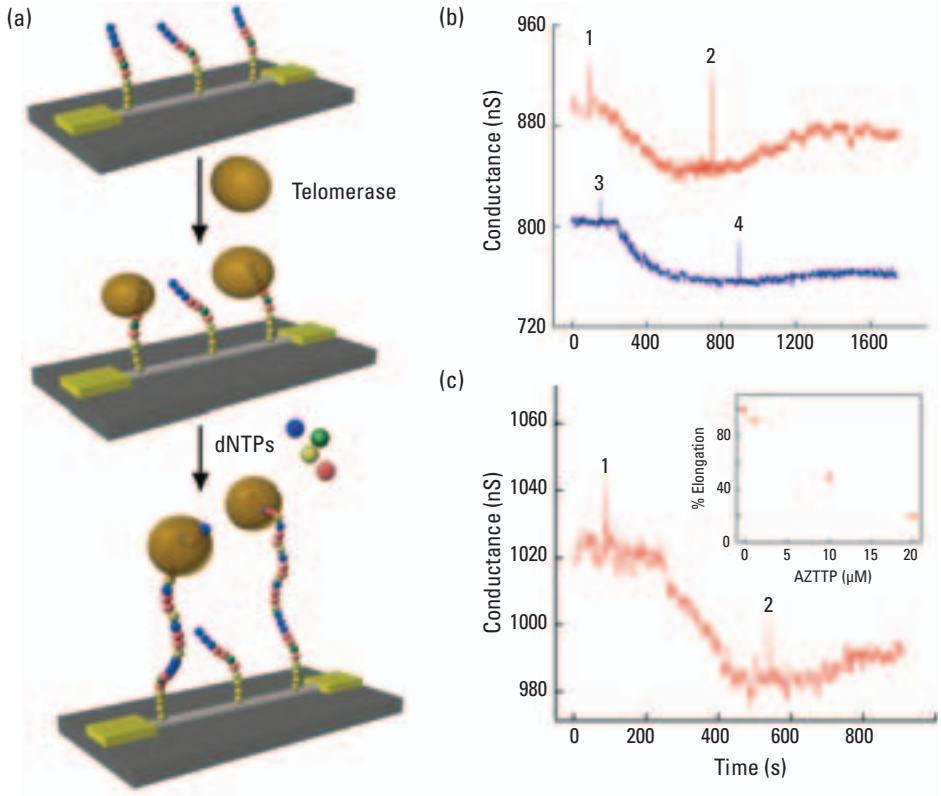

FIGURE 4. Real-time detection of DNA and DNA reactions.

(a) Schematic of telomerase binding and activity assay. (b) Conductance vs time for oligonucleotide-modified p-SiNW devices after the introduction of solutions containing (points 1 and 3) extract from 100 HeLa cells, (point 2) all 4 dNTPs, and (point 4) deoxycytosine triphosphate only. (c) Conductance vs time after the introduction of solutions containing (point 1) extract from 100 HeLa cells and (point 2) all 4 dNTPs, each at 0.1 mM, and 20-μM AZTTP. Inset is a plot of the inhibition of elongation vs AZTTP concentration.

Conductance data recorded from p-SiNWs modified with oligonucleotide primers showed well-defined conductance decreases after delivery of the HeLa cell extract (points 1 and 3, Figure 4b). These decreases corresponded to the selective binding of the positively charged telomerase at the surfaces of the NWs in the array (*29*). Notably, concentration-dependent studies showed that binding was readily detectable to at least the 10-cell level without amplification. No signal was observed with an extract from 100,000 normal human fibroblast cells or heat-denatured HeLa cell extracts; this suggests that the signal is specific to the presence of active telomerase (*29*). The primer-modified NW arrays were also effective in monitoring the enzyme's activity (point 2, Figure 4b). After initial telomerase binding, dNTPs were added, and an increase in the device's conductance was observed. The increase can be explained by the incorporation of negatively charged nucleotide units on the NW surface during the telomerase-catalyzed process. This conclusion is strongly supported by several control experiments (*29*), which demonstrated that no significant conductance increase was observed after the telomerase binding step in the absence of dNTPs (point 4, Figure 4b). These measurements were all carried out in solutions with relatively high (millimolar) ionic strength and, thus, show that NW sensors are not restricted to low-ionic-strength conditions.

Significantly, our telomerase activity measurements are distinct from and advantageous compared to current approaches (*46*, *47*) because our approach does not require PCR amplification to achieve high sensitivity. In addition, the fact that telomerase inhibitors can be directly screened speaks to the versatility of NW detectors and of our telomerase assay. This point was demonstrated clearly through investigations of the inhibition of telomerase elongation activity in the presence of azido deoxythymidine triphosphate (AZTTP; *29*, *48*), a known reverse transcriptase inhibitor (*29*, *48*; Figure 4c). Taken together, these studies clearly show the sensitivity and selectivity of NW sensors for telomerase detection and activity in biological cells.

Multiplexed real-time detection of proteins

In 2001, the first example of electrical detection of proteins in solution with nanostructures was reported by our group with p-SiNW devices (*23*). Biotin, which binds with high selectivity to streptavidin, was linked to the oxide surface of the NWs and used as a binding receptor. When solutions of streptavidin were delivered to NW sensor devices modified with biotin receptors, the conductance increased rapidly to a constant value and was stable after the addition of pure buffer solution. These results were consistent with the net negative charge on streptavidin at the pH of these experiments (i.e., causing accumulation of carriers in the p-SiNWs) and the very low dissociation rate of the streptavidin–biotin complex, respectively.

More recently, we explored the use of NW devices for the detection of multiple proteins simultaneously in a single, versatile detection platform (*29*). One important application is the multiplexed detection of protein biomarkers, which are thought to have the potential to greatly improve the diagnosis of diseases (*49*). The availability of multiple biomarkers is believed to be especially important in the diagnosis of complex cancers because disease heterogeneity makes single-marker tests, such as the analysis of prostate-specific antigen (PSA), inadequate (*50*). The analysis of patterns of multiple cancer markers might provide the information necessary for robust diagnosis of any person within a population (*51*). Moreover, detection of markers associated with different stages of disease pathogenesis could further facilitate early detection, which is especially important for successful cancer treatment.

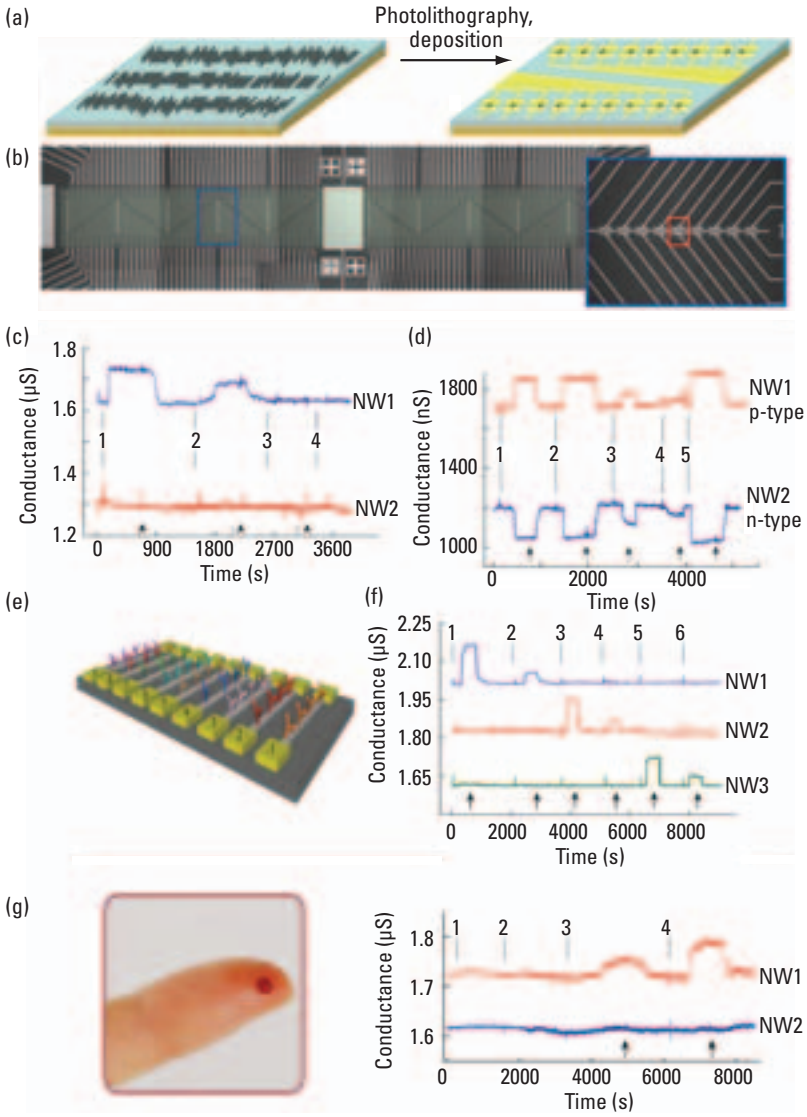

FIGURE 5. NW arrays for multiplexed protein sensing.

(a) Illustration of NW array fabrication. (b) Optical image of a portion of a NW array; the blue boxes show one row of individually addressable elements; the red box highlights a single device. (c) Data recorded simultaneously from 2 p-SiNW devices; NW1 was functionalized with PSA-Ab1, and NW2 was modified with ethanolamine. Vertical lines correspond to times when solutions of (point 1) 9 pg/mL PSA, (point 2) 1 pg/mL PSA, (point 3) 10 μg/mL BSA, and (point 4) a mixture of 1 ng/mL PSA and 10 μg/mL PSA-Ab1 were added. Black arrows correspond to the points at which the solution was switched to buffer in (c), (d), (f), and (g). (d) Complementary sensing of PSA with p-type (NW1) and n-type (NW2) NW devices. Vertical lines correspond to addition of PSA solutions of (points 1 and 2) 0.9 ng/mL, (point 3) 9 pg/mL, (point 4) 0.9 pg/mL, and (point 5) 5 ng/mL. (e) Schematic of array detection of multiple proteins. (f) Simultaneous detection of PSA, CEA, and mucin-1 with NW1, NW2, and NW3 functionalized with antibodies for these compounds. Protein solutions of (points 1 and 2) PSA, (points 3 and 4) CEA, and (points 5 and 6) mucin-1 were delivered sequentially to the array. (g) The drop of blood on this finger corresponds roughly to the quantity required for analysis. Conductance vs time data recorded for the detection of PSA in donkey serum samples with (point 1) buffer, (point 2) serum, and (points 3 and 4) serum and PSA. NW2 was passivated with ethanolamine.

We fabricated electrically addressable arrays by a process that uses fluid-based assembly of NWs to align them and set their average spacing over large areas (*11*, *20*, *52*, *53*). Photolithography and metal deposition define interconnections to a large number of individual NWs in parallel (Figure 5a). A key feature of this approach is that the metal electrodes defined by conventional lithography do not need to be registered to individual NWs in an array to achieve a high yield of devices; only the position of the electrodes relative to a group of aligned NWs needs to be fixed. An example containing >100 independently electrically addressable devices is shown in Figure 5b. The active NW sensor devices are confined to a central rectangular area that overlaps with the microfluidic sample delivery channel (green). Critical to the success of any integrated nanoelectronic array is the reproducibility of the device elements within the array. Measurements made on NW FET arrays have demonstrated very reproducible, high-performance properties (*20*, *53*).

As a first step, the single biomarker PSA was detected by modifying NW elements with the monoclonal antibody PSA-Ab1. Sensitivity limits were determined by measuring conductance changes as the solution concentration of PSA was varied. Figure 5c (NW1) shows a well-defined conductance increase and a subsequent return to baseline when PSA solution (point 1) and pure buffer (point 2) are alternately delivered through the microfluidic channel to the devices. Notably, these data show that direct detection of PSA is routinely achieved with S/N >3 for concentrations down to 75 fg/mL or ~2 fM (*29*).

The reproducibility and selectivity of the NW devices were further demonstrated in competitive binding experiments (Figure 5c, points 3 and 4), in which no conductance changes were observed after delivery of concentrated bovine serum albumin (BSA) solutions or solutions containing both PSA and PSA-Ab1 (to pre-block PSA). Our basic array design enables the incorporation of different types of addressable NWs, so a second control was carried out in parallel with a p-SiNW device passivated with ethanolamine (NW2, Figure 5c). Simultaneous measurements of NW1 and NW2 show that well-defined concentration-dependent conductance increases were only observed in NW1 upon delivery of PSA solutions; no response was observed for NW2. This simple implementation of multiplexing represents a robust means for discriminating against false positive signals arising from either electronic noise or nonspecific binding (*29*).

In another demonstration of the multiplexing capability of the arrays, distinct p-type (NW1) and n-type (NW2) device elements were incorporated in a single sensor chip. The data recorded simultaneously from both device types (Figure 5d) show an increase/decrease in conductance when PSA solution is delivered to the p-type/n-type devices and a subsequent return to the baseline with the delivery of buffer. The complementary electrical signals provide a

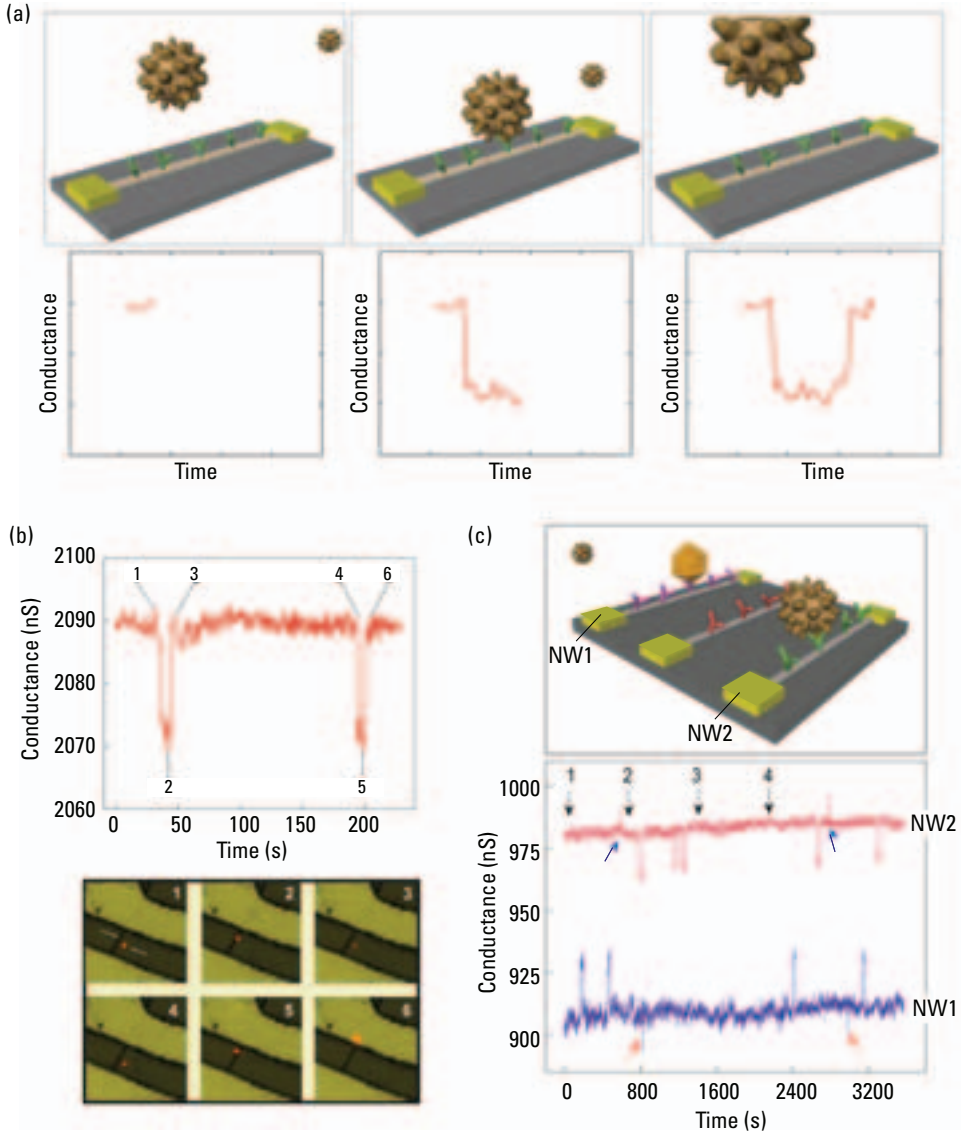

FIGURE 6. Detection of single viruses.

(a) Schematic of a single virus particle binding to and unbinding from the surface of a SiNW device that was modified with antibody receptors. For each step, the corresponding time-dependent change in conductance is shown. (b) Simultaneous conductance and optical data recorded for a SiNW device after the introduction of influenza A solution. (c) Schematic of multiplexed single-virus detection. Conductance vs time recorded simultaneously from NW2, which was modified with antibody for influenza A (red), and NW1, which was modified with antibody for adenovirus (blue). Black arrows 1–4 correspond to the introduction of adenovirus, influenza A, pure buffer, and a 1:1 mixture of adenovirus and influenza A. Small red and blue arrows highlight conductance changes corresponding to the diffusion of viral particles past the NW surface without specific binding for influenza and adenovirus, respectively.

simple yet robust means for detecting false positive signals from electrical noise or nonspecific binding of protein: Real and selective binding events must show complementary responses in the p- and n-type devices. The presence of correlated conductance signals, which occur at points when the buffer and PSA–buffer solutions are changed, in both devices clearly illustrates how this multiplexing capability can be used to distinguish noise from protein binding signals (*29*).

Finally, multiplexed detection of distinct marker proteins, to facilitate pattern analysis for diagnosis (*51*), can be carried out with high sensitivity and selectivity with NW arrays modified with distinct antibody receptors (Figure 5e). Different receptors can be selectively deposited on the different areas of a sensor array chip by the microarray technique widely used for proteomics studies (*54*). SiNW devices functionalized with monoclonal antibody receptors for PSA (NW1), carcinoembryonic antigen (CEA; NW2), and mucin-1 (NW3; *29*) were used to demonstrate this critical capability. Conductance measurements were recorded simultaneously from NW1, NW2, and NW3 as different protein solutions were sequentially delivered to the device array. The result was multiplexed, real-time, label-free detection of marker proteins with sensitivity to the femtomolar level and ~100% selectivity (Figure 5f).

Effective cancer diagnosis will require rapid analysis of clinically relevant samples, such as blood serum. A key test of NW arrays, therefore, is their performance when confronted with such a real-world sample. We studied PSA in undiluted serum samples that were desalted in a rapid and simple purification step (*29*). The desalting step was necessary to reduce solution ionic strength to achieve high detection sensitivity. Conductance versus time was recorded simultaneously from NW1, which was modified with PSA-Ab1 receptor, and NW2, which was passivated with ethanolamine. Serum that contained 59 mg/mL total protein (without PSA) did not lead to an appreciable conductance change relative to the standard assay buffer; however, serum that contained PSA led to concentration-dependent conductance increases only for NW1 (Figure 5g). Well-defined conductance changes were observed for PSA concentrations as low as 0.9 pg/mL, which corresponds to a concentration 100 billion times lower than that of the background proteins in the sample. Taken together, these results strongly suggest that NW sensor arrays can be used to detect multiple cancer markers rapidly with high sensitivity and selectivity in undiluted human serum. Note that the detection can be carried out on as little as a drop of blood instead of the several milliliters needed for current analyses.

Pushing sensitivity: Detecting single viruses

Although these studies show exquisite sensitivity unmatched by existing label-free sensor devices, they do not define the ultimate sensitivity of NW FET devices. To address this critical issue, our group recently studied the detection of viruses, which are among the most important causes of human disease and are agents for biological warfare and terrorism (*55*, *56*). Our goal was to determine whether the ultimate limit of one single entity could be reliably detected (*28*).

The fact that these nanowire sensors transduce chemical and biological binding events into electronic and digital signals suggests the potential for a highly sophisticated interface between nanoelectronic and biological information processing systems.

The underlying concept of our experiments is illustrated in Figure 6a. When a virus particle binds to the antibody receptor on a NW device, the conductance of that device will change from the baseline value; when the virus unbinds, the conductance will return to the baseline. Significantly, delivery of highly dilute influenza A virus solutions, ~80 aM or 50 viruses/mL, to p-SiNW devices modified with monoclonal antibody for influenza A produced well-defined, discrete conductance changes (Figure 6b) that are characteristic of the binding and unbinding of a single positively charged influenza particle (*28*).

Definitive proof that the discrete conductance changes observed in these studies were due to detection of the binding and unbinding of an individual entity was obtained from simultaneous optical and electrical measurements with fluorescently labeled influenza viruses (Figure 6b). These data showed that as a virus diffused near a NW device, the conductance remained at the baseline, and only after the virus bound at the NW surface did the conductance drop in a quantized manner similar to that observed with unlabeled viruses; as the virus unbound and diffused from the NW surface, the conductance returned rapidly to the baseline. These parallel measurements also showed that a virus had to be in contact with the NW device for an electrical response to be obtained. This result suggests that it will be possible to develop ultradense NW device arrays without cross talk, where the minimum scale is set by the size of the virus.

The initial multiplexing experiments consisted of different, multiple NW sensors modified with antibody receptors specific for different viruses (*28*). Specifically, p-SiNW devices were modified with monoclonal antibody receptors specific for either influenza A (NW2) or adenovirus (NW1). Simultaneous conductance measurements were obtained when adenovirus, influenza A, and a mixture of both were delivered to the devices (Figure 6c). First, delivery of adenovirus, which is negatively charged at the pH of the experiment, yielded positive conductance changes for NW1; the "on" time was similar to that for the selective binding and unbinding in single-device experiments. As expected, well-defined binding and unbinding events were not observed from the NW device modified with the influenza A virus receptor (NW2).

Second, delivery of influenza A solutions yielded negative conductance changes for NW2, similar to single-device measurements in Figure 6b, whereas well-defined binding and unbinding events were not observed on NW1. Finally, in a mixture of both viruses, selective binding and unbinding responses for adenovirus and influenza A were unambiguously detected in parallel by NW1 and NW2, respectively, at the single-virus level.

Conclusions and future directions

We have shown that NW-based field-effect sensor devices modified with specific surface receptors represent a powerful detection platform for a broad range of biological and chemical species in solution. Several key features set these devices apart from other sensor technologies available today: direct, label-free, real-time electrical signal transduction; ultrahigh sensitivity; exquisite selectivity; and the potential for integration of addressable arrays. The examples described in this article show clearly the potential of these devices to significantly impact disease diagnosis, genetic screening, and drug discovery as well as serve as powerful new tools for research in many areas of biology.

However, some limitations also exist. An intrinsic limitation of field-effect devices is that the detection sensitivity depends on solution ionic strength. Because blood serum samples have high ionic strength, diagnostics will require a simple desalting step before analysis to achieve the highest sensitivity (*29*). A practical constraint of this technique for other research groups might be the fact that the synthesis and fabrication of NW biosensor devices require some technologies that are not common to traditional analytical chemistry and biology laboratories. However, with the increasingly common interdisciplinary nature of research within academics and industry, we believe that the methods for device fabrication will be within reach. We predict that more groups will eventually be able to exploit this technology through development of expertise within their laboratories or collaboration.

In addition, we believe that these advances could be developed at the commercial level in simple NW sensor devices that would represent a clear application of nanotechnology. For example, advances in capabilities of assembling larger and more complex NW sensor arrays and integrating them first with conventional and later with nanoscale electronics for processing will lead to exquisitely powerful sensor systems that could enable the dream of personalized medicine. Moreover, the fact that these NW sensors transduce chemical and biological binding events into electronic and digital signals suggests the potential for a highly sophisticated interface between nanoelectronic and biological information processing systems.

We graciously thank the scientists cited in this article for their contributions to the research. Lieber acknowledges generous support from the Defense Advanced Research Projects Agency, the National Cancer Institute, Applied Biosystems, and the Ellison Medical Foundation.

Fernando Patolsky is a postdoctoral fellow, Gengfeng Zheng is a graduate student, and Charles M. Lieber is a professor at Harvard University. Patolsky works in the field of bionanotechnology and develops SiNW-based FET devices for biosensing applications. Zheng builds highly sensitive NW-based arrays for detecting biomolecules. Lieber's research focuses on the chemistry and physics of nanoscale materials, including rational synthesis of NWs and NW heterostructures and the hierarchical assembly of nanoscale materials into complex and functional systems; applications include electrically based biological detection, interfaces between digital and biological information processing systems, and electrical and photonic-based computing. Address correspondence to Lieber at 12 Oxford St., Cambridge, MA 02138 (cml@cmliris.harvard.edu).

References

(1) Ward, A. M.; Catto, J. W. F.; Hamdy, F. C. *Ann. Clin. Biochem.* **2001**, *38*, 633–651.
(2) Campagnolo, C.; et al. *J. Biochem. Biophys. Methods* **2004**, *61*, 283–298.
(3) Mirkin, C. A.; et al. *Nature* **1996**, *382*, 607–609.
(4) Domansky, K.; Janata, J. *Analyst* **1993**, *118*, 335–340.
(5) Janata, J. *Analyst* **1994**, *119*, 2275–2278.
(6) Wu, G. H.; et al. *Nat. Biotechnol.* **2001**, *19*, 856–860.
(7) Chen, R. J.; et al. *Proc. Natl. Acad. Sci. U.S.A.* **2003**, *100*, 4984–4989.
(8) Chen, R. J.; et al. *J. Am. Chem. Soc.* **2004**, *126*, 1563–1568.
(9) Morales, A. M.; Lieber, C. M. *Science* **1998**, *279*, 208–211.
(10) Hu, J. T.; Odom, T. W.; Lieber, C. M. *Acc. Chem. Res.* **1999**, *32*, 435–445.
(11) Lieber, C. M. *MRS Bull.* **2003**, *28* (7), 486–491.
(12) Wang, Z. L. *Mater. Today* **2004**, *7* (6), 26–33.
(13) Chan, W. C. W.; et al. *Curr. Opin. Biotechnol.* **2002**, *13*, 40–46.
(14) Alivisatos, P. *Nat. Biotechnol.* **2004**, *22*, 47–52.
(15) Duan, X. F.; et al. *Nature* **2001**, *409*, 66–69.
(16) Cui, Y.; Lieber, C. M. *Science* **2001**, *291*, 851–853.
(17) Gudiksen, M. S.; et al. *Nature* **2002**, *415*, 617–620.
(18) Cui, Y.; et al. *Nano Lett.* **2003**, *3*, 149–152.
(19) Thelander, C.; et al. *Appl. Phys. Lett.* **2003**, *83*, 2052–2054.
(20) Jin, S.; et al. *Nano Lett.* **2004**, *4*, 915–919.
(21) Wu, Y.; et al. *Nature* **2004**, *430*, 61–65.
(22) Zheng, G. F.; et al. *Adv. Mater.* **2004**, *16*, 1890–1894.
(23) Cui, Y.; et al. *Science* **2001**, *293*, 1289–1292.
(24) Comini, E.; et al. *Appl. Phys. Lett.* **2002**, *81*, 1869–1871.
(25) Patolsky, F.; Lieber, C. M. *Mater. Today* **2005**, *8*, 20–28.
(26) Hahm, J.; Lieber, C. M. *Nano Lett.* **2004**, *4*, 51–54.
(27) Wang, W. U.; et al. *Proc. Natl. Acad. Sci. U.S.A.* **2005**, *102*, 3208–3212.
(28) Patolsky, F.; et al. *Proc. Natl. Acad. Sci. U.S.A.* **2004**, *101*, 14,017–14,022.
(29) Zheng, G. F.; et al. *Nat. Biotechnol.* **2005**, *23*, 1294–1301.
(30) Li, C.; et al. *J. Am. Chem. Soc.* **2005**, *127*, 12,484–12,485.
(31) Streifer, J. A.; et al. *Nanotechnology* **2005**, *16*, 1868–1873.
(32) Sze, S. M. *Physics of Semiconductor Devices*; Wiley: New York, 1981; p 431.
(33) Bergveld, P. *IEEE Trans. Biomed. Eng.* **1972**, *BME–19*, 342.
(34) Blackburn, G. F. In *Biosensors: Fundamentals and Applications*; Turner, A. P. F., Karube, I., Wilson, G. S., Eds.; Oxford University Press: Oxford, UK, 1987; p 481.
(35) Wu, Y.; et al. *Nano Lett.* **2004**, *4*, 433–436.
(36) Bartlett, P. N. In *Handbook of Chemical and Biological Sensors*; Taylor, R. F., Schultz, J. S., Eds.; IOP Publishing: Philadelphia, PA, 1996, p 139.
(37) Bolt, G. H. *J. Phys. Chem.* **1957**, *61*, 1166–1170.
(38) Strausberg, R. L.; Schreiber, S. L. *Science* **2003**, *300*, 294–295.
(39) Becker, J. *Nat. Biotechnol.* **2004**, *22*, 15–18.
(40) Jensen, K. K.; et al. *Biochemistry* **1997**, *36*, 5072–5077.
(41) He, L.; et al. *J. Am. Chem. Soc.* **2000**, *122*, 9071–9077.
(42) Mao, X. L.; et al. *Biosens. Bioelectron.* **2006**, *21*, 1178–1185.
(43) Moyzis, R. K.; et al. *Proc. Natl. Acad. Sci. U.S.A.* **1988**, *85*, 6622–6626.
(44) O'Reilly, M.; Teichmann, S. A.; Rhodes, D. *Curr. Opin. Struct. Biol.* **1999**, *9*, 56–65.
(45) Kim, N. W.; et al. *Science* **1994**, *266*, 2011–2015.
(46) Szatmari, I.; et al. *Anal. Biochem.* **2000**, *282*, 80–88.
(47) Wege, H.; et al. *Nucleic Acids Res.* **2003**, *31* (2), e3.
(48) Mitsuya, H.; Yarchoan, R.; Broder, S. *Science* **1990**, *9*, 1533–1544.
(49) Etzioni, R.; et al. *Nat. Rev. Cancer* **2003**, *3*, 1–10.
(50) Wulfkuhle, J. D.; Liotta, L. A.; Petricoin, E. F. *Nat. Rev. Cancer* **2003**, *3*, 267–275.
(51) Sidransky, D. *Nat. Rev. Cancer* **2002**, *2*, 210–219.
(52) Huang, Y.; et al. *Science* **2001**, *291*, 630–633.
(53) Whang, D.; Jin, S.; Lieber, C. M. *Jpn. J. Appl. Phys.* **2004**, *43*, 4465–4470.
(54) MacBeath, G.; Schreiber, S. L. *Science* **2000**, *289*, 1760–1763.
(55) Stadler, K.; et al. *Nat. Rev. Microbiol.* **2003**, *1*, 209–218.
(56) Atlas, R. M. *Nat. Rev. Microbiol.* **2003**, *1*, 70–74.